Analysis of Serotonin *N*-Acetyltransferase Regulation in Vitro and in Live Cells Using Protein Semisynthesis[†]

Lawrence M. Szewczuk, Mary K. Tarrant, Vedangi Sample, William J. Drury III, Jin Zhang, and Philip A. Cole*

Department of Pharmacology and Molecular Sciences, Johns Hopkins University School of Medicine, Baltimore, Maryland 21205

Received June 25, 2008; Revised Manuscript Received August 5, 2008

ABSTRACT: Serotonin *N*-acetyltransferase [arylalkylamine *N*-acetyltransferase (AANAT)] is a key circadian rhythm enzyme that drives the nocturnal production of melatonin in the pineal. Prior studies have suggested that its light and diurnal regulation involves phosphorylation on key AANAT Ser and Thr residues which results in 14-3-3ζ recruitment and changes in catalytic activity and protein stability. Here we use protein semisynthesis by expressed protein ligation to systematically explore the effects of single and dual phosphorylation of AANAT on acetyltransferase activity and relative affinity for 14-3-3ζ. AANAT Thr31 phosphorylation on its own can enhance catalytic efficiency up to 7-fold through an interaction with 14-3-3ζ that lowers the substrate K_m. This augmented catalytic profile is largely abolished by double phosphorylation at Thr31 and Ser205. A possible basis for this difference is the dual anchoring of doubly phosphorylated AANAT via one 14-3-3ζ heterodimer. We have developed a novel solution phase assay for accurate K_D measurements of 14-3-3ζ−AANAT interaction using 14-3-3ζ fluorescently labeled with rhodamine by expressed protein ligation. We have also generated a doubly fluorescently labeled AANAT which can be used to assess the stability of this protein in a live cell, real-time assay by fluorescence resonance energy transfer measured by microscopic imaging. These studies offer new insights into the molecular basis of melatonin regulation and 14-3-3ζ interaction.

Melatonin is a key circadian rhythm hormone that is produced in a diurnal pattern, driven by changes in the level of the biosynthetic enzyme serotonin *N*-acetyltransferase [arylalkylamine *N*-acetyltransferase (AANAT)][1] (*1, 2*). The neuroendocrine network responsible for modulating AANAT levels has been intensively investigated, and some aspects of this regulation are now understood. Light detected by the retina results in neurotransmission through the suprachiasmatic nucleus that in turn induces a drop in norepinephrine stimulation to the pineal (*1, 2*). Norepinephrine activates the adrenergic receptor which in turn stimulates a protein kinase A (PKA) signaling cascade, which results in AANAT being phosphorylated on two sites by PKA (*3*−*5*). It is believed that AANAT phosphorylation at Thr31 and Ser205 enhances its interaction with 14-3-3ζ which appears to stabilize AANAT against degradation (*3*−*6*). Moreover, recruitment of 14-3-3ζ to AANAT has also been suggested to modulate its acetyltransferase activity (*3*−*6*). However, the precise details of how each phosphorylation site in AANAT contributes to 14-3-3ζ recruitment and affinity have not yet been settled. Although the stability of AANAT has been studied in fixed cell assays by immunocytochemistry (*7, 8*), it would be advantageous to demonstrate real-time sensitivity to proteolytic breakdown in live cells.

In this study, we use protein semisynthesis employing the native chemical ligation reaction to investigate these questions. In this approach, peptides and/or proteins containing $^{\alpha}$thioesters are reacted with peptides and/or proteins bearing N-terminal Cys residues in a chemoselective reaction resulting in peptide bond formation (*9*−*12*) (Scheme 1). In previous applications of this semisynthetic method to AANAT, phosphorylated residues (pSer and pThr) or nonhydrolyzable mimics were installed at the two sites of phosphorylation of AANAT, and it was demonstrated that these modified proteins can resist intracellular breakdown after microinjection (*13, 14*). Here we use protein semisynthesis to prepare doubly phosphorylated (pThr31 and pSer205) AANAT and assess the effects on 14-3-3ζ binding and acetyltransferase

[†] Supported by the NIH.

* To whom correspondence should be addressed. E-mail: pcole@jhmi.edu. Telephone: (410) 614-8849. Fax: (410) 614-7717.

[1] Abbreviations: PKA, protein kinase A; AANAT, arylalkylamine *N*-acetyltransferase or serotonin *N*-acetyltransferase; GST, glutathione *S*-transferase; FRET, fluorescence resonance energy transfer; HEPES, hydroxyethylpiperazineethanesulfonate; DTT, dithiothreitol; EDTA, ethylenediaminetetraacetate; NMM, *N*-methylmorpholine; MPAA, mercaptophenylacetic acid; MESNA, mercaptoethane sulfonate sodium; ss-WT, semisynthetic wild-type AANAT (see Figure 1); ss-pS205, semisynthetic AANAT containing a pSer at position 205 (see Figure 1); ss-pT31, semisynthetic AANAT containing a pSer at position 31 (see Figure 1); ss-pT31-pS205, semisynthetic AANAT containing a pThr at position 31 and a pSer at position 205 (see Figure 1); Δ-CD, C-terminally deleted recombinant AANAT amino acids 1−198; ss-GC-Insert, semisynthetic AANAT using C-terminal ligation and GC inserted between amino acids 33 and 34 recombinantly (see Figure 1); ss-14-3-3ζ-Rh, semisynthetic 14-3-3ζ linked to rhodamine (see Figure 1); ss-WT/PKA, ss-WT treated with protein kinase A (see Figure 2); ss-pS205/PKA, ss-p205 treated with protein kinase A (see Figure 2); ss-pT31-pS205/PKA, ss-pT31-pS205 treated with protein kinase A (see Figure 2); ss-pS205/PKA, ss-pS205 treated with protein kinase A (see Figure 2); ΔC8/PKA, ΔC8 treated with protein kinase A (see Figure 2); ss-GC-Insert/PKA, ss-GC-Insert treated with protein kinase A (see Figure 2); Fl-AANAT-Rh, semisynthetic AANAT containing an N-terminal fluorescein and a C-terminal rhodamine; EPL, expressed protein ligation.

10.1021/bi801189d CCC: $40.75
Published on Web 09/05/2008

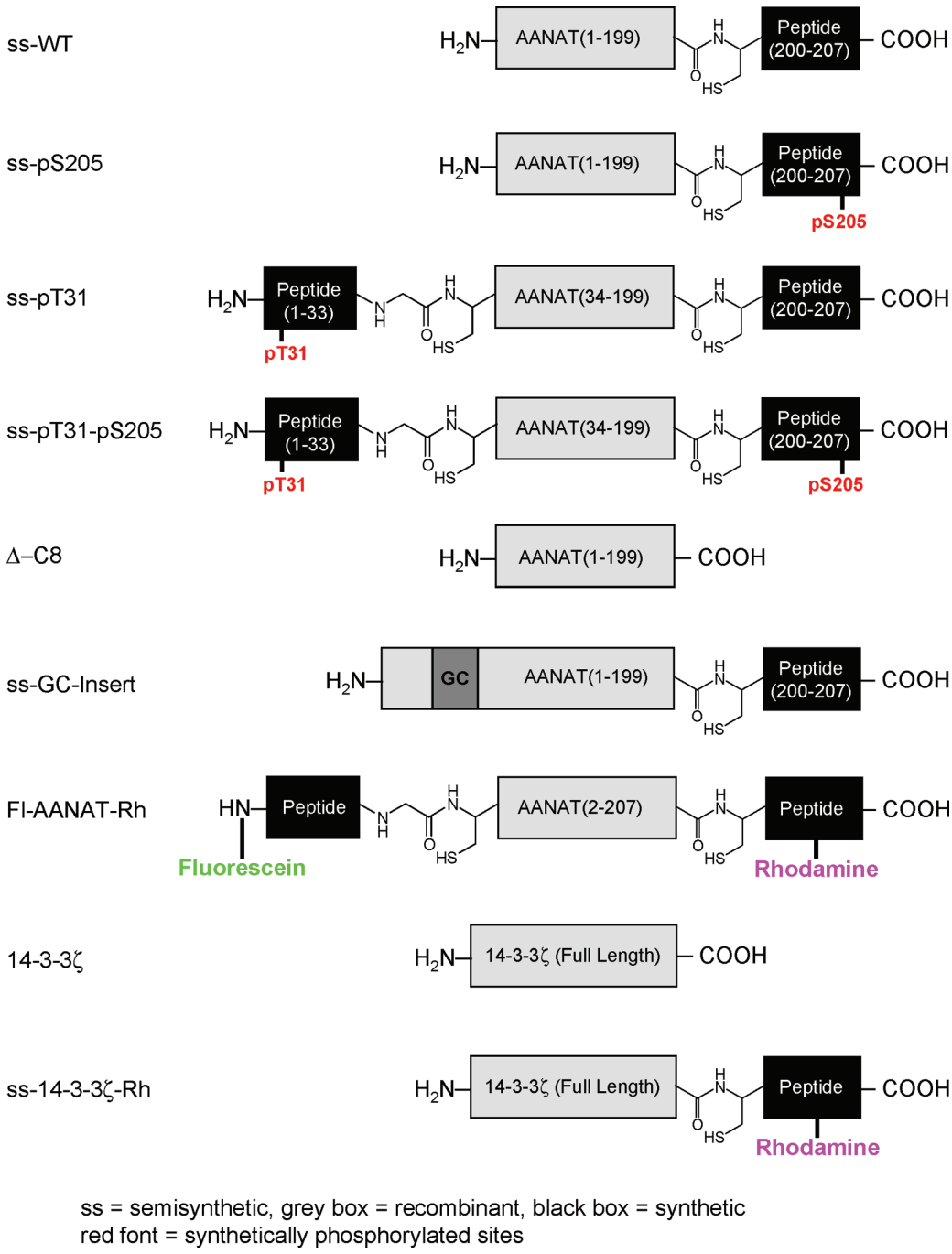

FIGURE 1: Proteins prepared for this study.

activity. We have also applied protein semisynthesis to generate a fluorescently labeled 14-3-3ζ that has proven to be useful for quantitative binding analysis of mono- and diphosphorylated AANAT by anisotropy. Finally, we employ protein semisynthesis to make FRET active doubly fluorescently labeled AANAT. This dually labeled protein allows for real-time measurement of proteolytic breakdown both in vitro and in cell culture. Taken together, these studies have exploited recently developed protein chemical methods to gain greater insight into the biochemical regulation of AANAT.

MATERIALS AND METHODS

Cloning and Expression of Proteins. AANAT 1−197 (ΔC8) and GST-AANAT 34−197 (ΔN33, ΔC8) were subcloned between the NdeI and SmaI sites of the pTYB2 intein expression vector (New England Biolabs). Then, the SmaI site was mutated (Quikchange, Stratagene) from PG to HA, which are the wild-type residues (amino acids 198 and 199) present in AANAT. Using the same methodology, a Factor Xa protease site followed by a Cys residue (IEGR-C) was introduced between the GST fusion and truncated AANAT. The resulting AANAT constructs were suitable for either two- or three-piece semisynthesis of full-length AANAT (1−207) as described in detail below. For FRET labeling, an AANAT ^{1}Cys-199-intein-chitin binding domain was subcloned into the pET-SUMO expression vector (Invitrogen), to be used in generating a protein that could be assembled in three pieces via semisynthetic methods. In addition, full-length 14-3-3ζ was subcloned between the NdeI

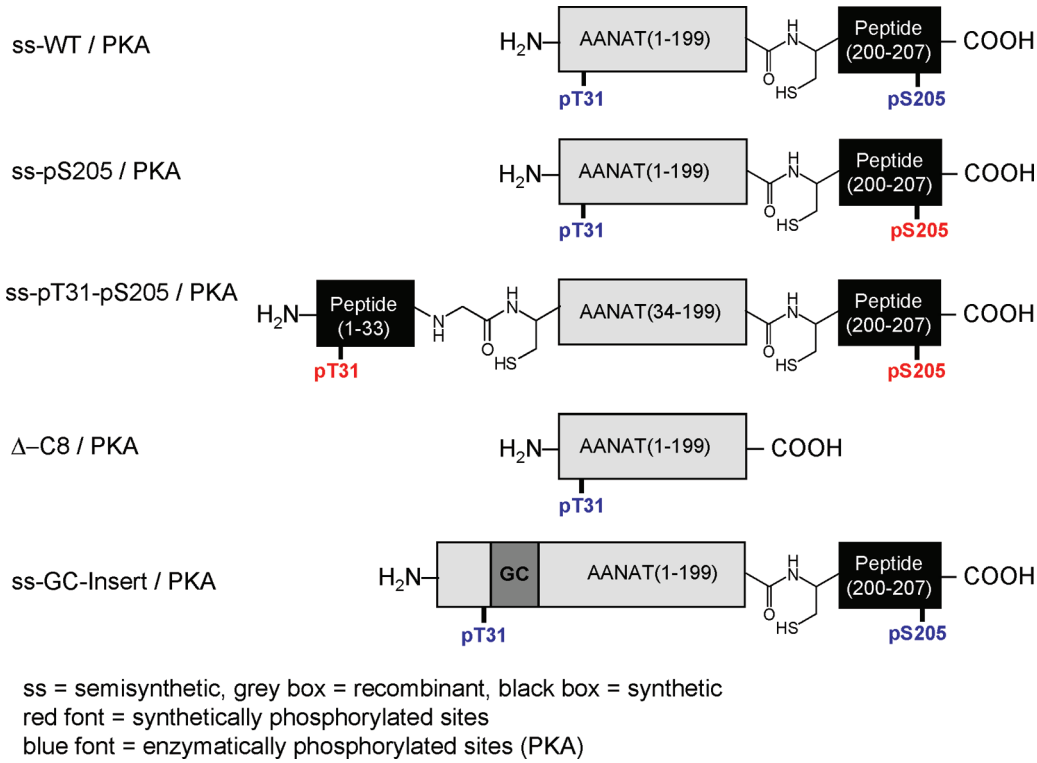

FIGURE 2: Proteins chemoenzymatically phosphorylated for this study.

and SmaI sites of the pTYB2 intein expression vector. In this case, the SmaI site was left intact, resulting in the production of a full-length 14-3-3ζ protein bearing an additional PG at its C-terminus (this additional dipeptide had no effect on protein behavior).

All proteins were overexpressed in *Escherichia coli* BL21-CodonPlus-DE3-RIPL cells (Stratagene). Cells were grown to an OD_{600} of 0.6 in LB medium at 37 °C, induced with 0.2 mM IPTG, and grown for 20 h at 16 °C. Cells were harvested by centrifugation at 5000*g* for 15 min and resuspended in ice-cold lysis buffer [50 mM HEPES (pH 7.5), 150 mM NaCl, 1 mM $MgSO_4$, 5% glycerol, and 5% ethylene glycol]. The cells were then lysed via a double pass on a French press (16000−18000 psi) and clarified by centrifugation at 25000*g* for 30 min (4 °C). The clarified lysate was then double loaded (0.5 mL/min) onto a pre-equilibrated chitin column (New England Biolabs). The column was then washed with 20 volumes of chitin column buffer [50 mM HEPES (pH 7.5), 250 mM NaCl, 1 mM EDTA, and 0.1% Triton X-100], followed by 10 volumes of ligation buffer [50 mM HEPES (pH 7.5), 250 mM NaCl, and 1 mM EDTA] at a flow rate of 1 mL/min. At this point, the immobilized proteins could be either cleaved from the chitin resin with DTT or ligated to a ^{1}Cys peptide. Cleavage was afforded by overnight treatment with 1 volume of 50 mM DTT in ligation buffer at room temperature followed by extensive dialysis into storage buffer [50 mM HEPES (pH 7.5), 150 mM NaCl, 1 mM EDTA, 10% glycerol, and 10 mM DTT]. In total, two proteins were cleaved from the resin using DTT and used for this study [ΔC8 and 14-3-3ζ (Figure 1)]. Ligation will be discussed in detail below. The mass and purity of all proteins (±50 Da) were confirmed via MALDI-MS and SDS−PAGE.

Peptide Synthesis. All Fmoc-protected amino acids and resins were obtained from Novabiochem. All peptides were assembled using a standard Fmoc solid phase peptide synthesis strategy on a Ranin PS-3 automated peptide synthesizer. ^{1}Cys peptides for C-terminal EPL were assembled on the Wang resin, where cleavage from the resin and global deprotection could be afforded by treatment with reagent K (87.5% TFA, 5% water, 5% thioanisole, and 2.5% ethanethiol). Two AANAT C-terminal ^{1}Cys peptides were synthesized for C-terminal expressed protein ligation: H_2N-CLRRNSDR-COOH and H_2N-CLRRN**pS**DR-COOH. Ligation of these peptides to the C-terminus of AANAT resulted in a single conservative point mutation (A200C).

The AANAT N-terminal pT31 peptide containing an $^{\alpha}$thioester (H_2N-MSTPSVHCLKPSPLHLPSGIPGSPGRQR-RH**pT**LPG-COS-benzyl) was synthesized by a modified Fmoc strategy with the C-terminal carboxylate derivatized in the solution phase followed by side chain deprotection with reagent K (*13*). A Gly residue was added to the C-terminus of the peptide sequence to eliminate epimerization at the C-terminal amino acid and to aid with ligation. Briefly, the peptides were assembled on the weak acid labile 2-chlorotrityl resin (2-Cl-Trt); then, the fully protected $^{\alpha}$carboxylate was cleaved from the resin with 25% hexafluoro-2-propanol, activated with diisopropylcarbodiimide, and coupled to benzyl mercaptan to yield the benzyl $^{\alpha}$thioester.

All deprotected peptides were precipitated and washed with cold diethyl ether and then lyophilized to yield crude peptide solids that were purified by preparative scale RP-HPLC using a water/acetonitrile gradient in the presence of 0.05% TFA. All peptides were obtained at >95% purity as judged by analytical RP-HPLC and MALDI-MS (data not shown).

Synthesis of Fluorescent Peptides. For C-terminal fluorescent labeling of both AANAT and 14-3-3ζ, the dipeptide H_2N-Cys-Lys(ε-rhodamine)-NH_2 was synthesized (*15*). Briefly, the dipeptide was assembled on the rink amide resin using

Scheme 1: Semisynthesis of AANAT

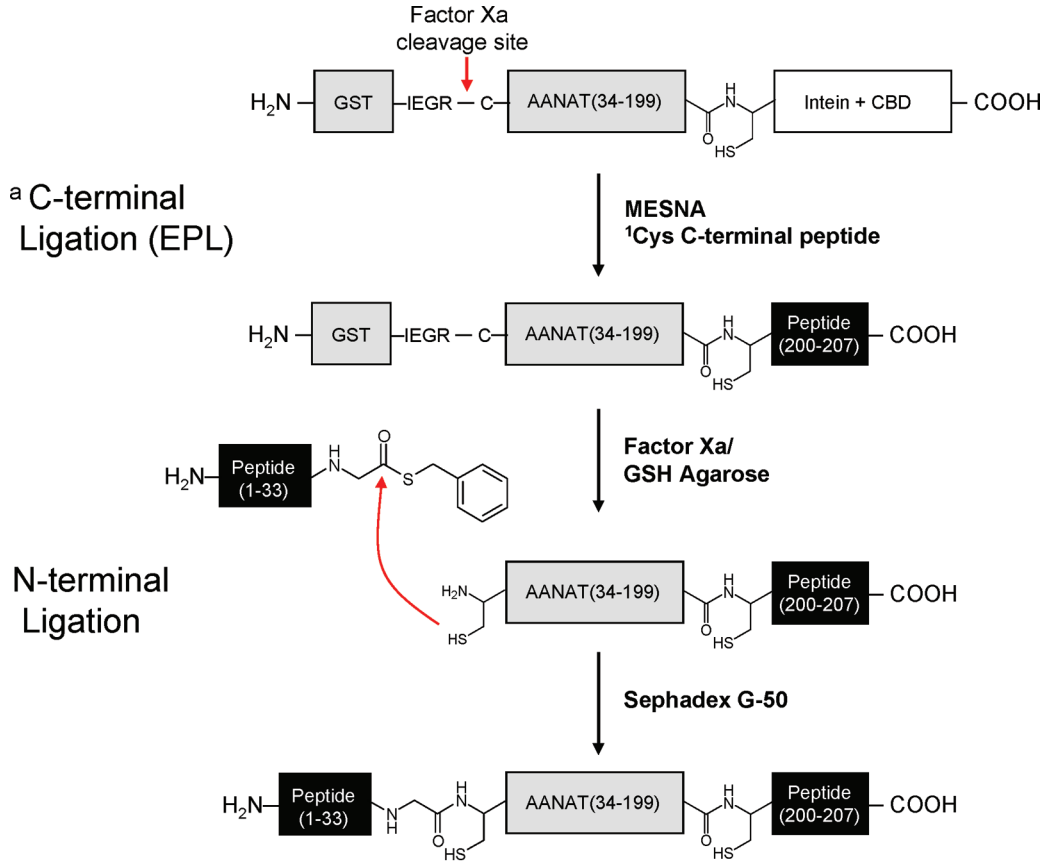

a = Proteins containing single C-terminal modifications (ss-WT, ss-pS205, ss-GC-Insert, and ss-14-3-3ζ-Rh) required only EPL

an orthogonally protected Lys derivative (ε-Dde) and Boc-Cys(Trt)-OH. After peptide assembly, the ε-amine was selectively deprotected with 2% hydrazine and reacted with NHS-rhodamine (Pierce) in DMF containing 0.4 M *N*-methylmorpholine (NMM). The peptide was cleaved from the resin, deprotected, and purified as described above.

To produce the reagent for N-terminal fluorescent labeling of AANAT, we assembled the dipeptide Fmoc-Lys(ε-Boc)-Gly on 4-sulfamylbutyryl-AM resin (loading the resin with Fmoc-Gly was achieved by following Novabiochem's outlined procedure). Briefly, the resin was preswollen in 10 volumes of dry methylene chloride for 1 h. During this period, Fmoc-Gly-OH (4 equiv) along with 1-methylimidazole (4 equiv) was dissolved in a 4:1 mixture of dry methylene chloride (DCM) and dimethylformamide (DMF) under a blanket of inert gas. To this clear colorless solution was added *N*,*N*′-diisopropylcarbodiimide (DIC). This solution was mixed for 5 min at room temperature, the resin drained, and the acylation mixture added to it. The resin solution was agitated for 18 h at room temperature and then drained. The resin was washed with portions of DCM, DMF, methanol, and *tert*-butyl-methyl ether prior to drying for subsequent use (*16*). The dipeptide was formed via standard manual peptide synthesis (deprotection with 20% piperidine in DMF, activation with HATU and Hünig's Base).

Following peptide assembly, the N-terminal Fmoc was removed with 20% piperidine in DMF, and the free amine reacted with NHS-fluorescein (Pierce) in DMF containing 0.4 M NMM. Next, the resin-bound sulfonamide was acylated with iodoacetonitrile and cleaved from the activated resin with mercaptophenyl acetic acid. Briefly, the resin (0.1 mmol) was preswollen in dry methylene chloride. During this period, a solution was made of iodoacetonitrile (25 equiv) and diisopropylethyl amine (10 equiv) in 3 mL of DMF and 1 mL of hexamethylphosphoric triamide. This dark solution was passed thought a column of activated basic alumina to provide a clear colorless solution. The swelling solvent was drained from the resin and the activation solution added. The solution was agitated in the dark for 18 h. At the end of this period, the solution was drained, and the resin was washed with portions of DMF, tetrahydrofuran, and DCM prior to immediate cleavage.

Finally, the fluorescein-labeled dipeptide was cleaved from the activated resin with mercaptophenylacetic acid and diisopropylethylamine in dichloromethane for 18 h at room temperature. In brief, the resin (0.1 mmol) was preswollen in dry DCM; during this period, a dry round-bottom flask was loaded with mercaptophenylacetic acid (2.0 mmol) and flushed with argon. The solid was suspended in DCM (10 mL) and cooled to 0 °C. To this was added dropwise Hünig's Base (1.0 mmol) over 5 min. This causes all of the solids to dissolve and the solution to become slightly yellow and clear. The resin was drained from the swelling solution and treated with the thiol solution. The resin bed was agitated in the dark for 18 h at room temperature. The bed was drained and the filtrate reserved. The bed was washed with three additional portions of DCM, these being pooled with the original filtrate. The organics were concentrated in vacuo to

provide a crude glass. The residue was treated with 10 mL of a 95:2.5:2.5 TFA/water/triisopropylsilane (TIS) mixture to remove the terminal Lys-ε-Boc group, and the peptide was filtered through Celite to remove excess insoluble thiol and concentrated in vacuo, followed by precipitation and washing with cold diethyl ether. The crude solid was dissolved in 25% acetonitrile with 0.1% TFA and lyophilized to dryness, and the crude peptide (fluorescein-Lys-Gly-COS-phenylacetic acid) was sufficiently pure to be used directly for ligation since only αthioester product could react with the ^{1}Cys protein. By leaving the Lys-ε-amine unmodified and preparing the MPAA αthioester, we were able to enhance solubility, since this compound would be zwitterionic under the neutral conditions required for native chemical ligation.

For anisotropy-based 14-3-3ζ competition binding studies, we selected a peptide sequence based on AANAT residues 19−38 which encompassed the pT31 14-3-3ζ binding motif (fluorescein-HN-GIPGSPGRQRRH**pT**LPANEFR-COOH) (*3*) and employed a standard Fmoc solid phase peptide synthesis strategy. Following peptide assembly, the N-terminal Fmoc group was removed with 20% piperidine in DMF and the free amine reacted with NHS-fluorescein in DMF containing 0.4 M NMM. The peptide was cleaved and purified as described above. The final purified peptide ligand was dissolved in water, and its concentration was determined by quantitative amino acid analysis (Harvard University Microchemistry).

Protein Semisynthesis. In total, seven semisynthetic proteins were prepared for this study, four by C-terminally expressed protein ligation (EPL) [ss-WT, ss-pS205, ss-GC-Insert, and ss-14-3-3ζ-Rh (Figure 1)] and three using a combination of C-terminal and N-terminal ligation [ss-pT31, ss-pT31-pS205, and Fl-AANAT-Rh (Figure 1)]. For C-terminal EPL (i.e., two-piece assembly), ligation was carried out with chitin resin-bound intein fusion protein for 3.5 days at room temperature in 1 column volume of 200 mM 2-mercaptoethanesulfonic acid sodium salt (MESNA) containing 2 mM ^{1}Cys peptide (Scheme 1). Released (ligated) proteins were then further purified by gel filtration (Sephadex G-50 in storage buffer) to remove excess free peptide. The ligated proteins were then concentrated, and the protein concentration was determined via a Bradford assay using BSA as the standard. For C-terminal rhodamine-labeled proteins, the concentration was determined by absorbance spectroscopy (ε_{558} = 60000 M^{-1} cm^{-1}) and confirmed by SDS−PAGE using the unlabeled protein as the standard.

For sequential three-piece assembly of semisynthetic AANAT, the GST-(Factor Xa)-AANAT 34−199 (ΔN33, ΔC8) construct was used. The first ligation, C-terminal EPL, was carried out as described above. Next, the GST tag was cleaved with 10 units of Factor Xa (GE Healthcare) per milligram of fusion protein. The reaction was allowed to proceed to ∼50% completion at 4 °C in Factor Xa cleavage buffer [50 mM Tris (pH 7.5), 150 mM NaCl, 1 mM $CaCl_2$, and 1 mM coenzyme A], conditions which reduced the level of formation of undesired degradation products. Factor Xa cleavage exposed an N-terminal Cys that would be used in the next ligation step. Free GST and Factor Xa were removed in a single step using a mixture of glutathione agarose and benzamidine agarose (Sigma). After purification, the proteins were extensively dialyzed into N-terminal ligation buffer [100 mM HEPES (pH 7.5), 500 mM NaCl, 5 mM EDTA, 1 mM benzamidine, and 5 mM MESNA] and then concentrated. N-Terminal ligation was achieved by mixing 12.5 equiv of peptide αthioester with ^{1}Cys-AANAT in N-terminal ligation buffer supplemented with 200 mM MESNA. The reaction was allowed to proceed for 20 h (>90% completion) and then the mixture immediately purified by gel filtration (Sephadex G-50 in storage buffer with 1 mM benzamidine) which led to the removal of free peptide and also separated the unligated AANAT. Semisynthetic AANAT prepared via three-piece assembly contained an extra Gly-Cys motif inserted into the protein framework (Gly from the peptide αthioester and Cys from the recombinant portion of the protein). From previous studies on semisynthetic AANAT, we knew that this insertion preserved the 14-3-3ζ binding elements (*13*). However, to thoroughly investigate the impact of this insertion and the N-terminal semisynthetic process, we generated a recombinant construct via Quikchange mutagenesis bearing the same Gly-Cys insert.

Assembly of FRET active AANAT (Fl-AANAT-Rh) was also performed using a sequential, three-piece strategy (Scheme 2). In this case, we used an N-terminal Sumo fusion protein which appeared to provide improved proteolytic selectivity. Again, C-terminal EPL was carried out first to ligate H_2N-Cys-Lys(ε-rhodamine)-NH_2 following the procedure for EPL described above. The ligated protein was extensively dialyzed against storage buffer and then concentrated. The Sumo fusion protein was cleaved using 15 units of Sumo protease (Invitrogen) per milligram of fusion protein. The reaction was allowed to proceed to completion at 4 °C in storage buffer supplemented with 500 mM NaCl and 2 mM coenzyme A. Immediately after cleavage, the digested protein was purified by gel filtration (Sephadex G-50 in N-terminal ligation buffer). AANAT-containing fractions were pooled, concentrated, mixed with 20 equiv of the fluorescein-Lys-Gly-MPAA αthioester reagent, and allowed to react for 20 h at room temperature in N-terminal ligation buffer supplemented with 200 mM MESNA. Immediately following ligation, Fl-AANAT-Rh was purified by gel filtration (Sephadex G-50 in storage buffer) to remove the free dipeptide. AANAT-containing fractions were pooled, concentrated, and purified by coenzyme A agarose (Sigma) to remove the Sumo fusion protein. The coenzyme A agarose column was loaded and washed in storage buffer diluted 1:10 with water [5 mM HEPES (pH 7.5), 15 mM NaCl, 0.1 mM EDTA, 0.5% glycerol, and 1 mM DTT]. Pure Fl-AANAT-Rh was eluted from the column in storage buffer supplemented with 500 mM NaCl and 1 mM coenzyme A.

Phosphorylation of Semisynthetic AANATs with PKA. To evaluate potential perturbation induced by the semisynthetic methodologies, we treated semisynthetic AANATs [ss-WT, ss-pS205, ss-pT31-pS205, ΔC8, and ss-GC-Insert (Figure 2)] with protein kinase A (Promega) and included them in our in vitro characterization of phosphorylated AANATs. The proteins were phosphorylated (in storage buffer supplemented with 20 mM Mg^{2+} acetate and 0.2−0.4 mM ATP) overnight at 4 °C using 500 units of protein kinase A per milligram of protein. Immediately following phosphorylation, the proteins were purified by gel filtration (Sephadex G-50 in storage buffer) to remove protein kinase A and ATP. Phosphorylation was confirmed by MALDI-MS, where the incorporation of one or two phosphates resulted in a mass change of +80 or +160 Da, respectively.

Scheme 2: Semisynthesis of FRET-Labeled AANAT

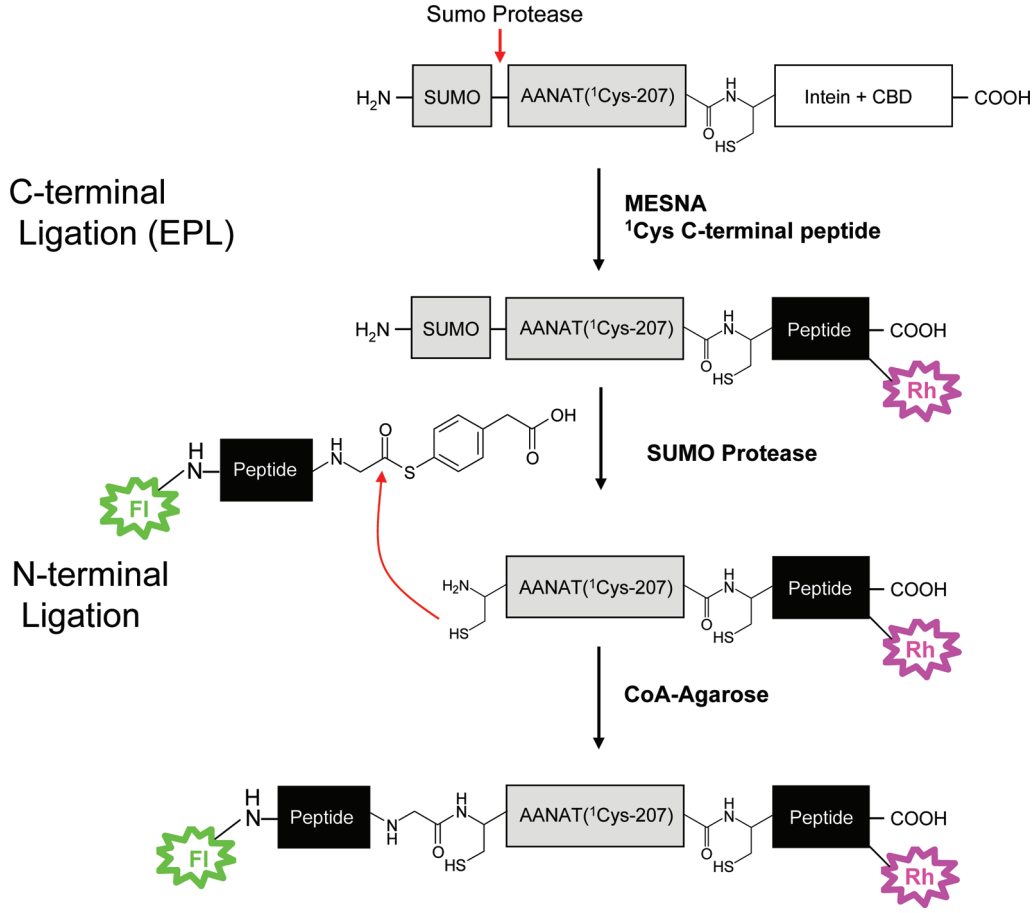

Kinetic Analysis of Semisynthetic AANATs. To determine the effects of AANAT phoshphorylation and 14-3-3ζ interaction on acetyltransferase activity, the previously developed DTNB assay (*17*) was used. Briefly, the reactions (200 μL) were carried out in 100 mM NH_4^+ acetate (pH 6.8) with 50 mM NaCl and 0.5 mM acetyl-coenzyme A (AcCoA, saturating), and the tryptamine concentration was varied (from 10 μM to 2.5 mM). The reactions were initiated with a final AANAT concentration of 1 nM, allowed to proceed for 2 min at 30 °C, and then quenched with 200 μL of 6 M guanidine HCl in assay buffer. DTNB was then added to the reaction mixture to produce a final concentration of 0.2 mM, and the absorbance at 412 nm was recorded. Reactions were linear over the time period measured and did not exceed 10% completion. End point absorbance values were converted to reaction rates using the extinction coefficient of the thiophenolate (ε_{412} = 13600 M^{-1} cm^{-1}), and the data were fit to the following equation to yield V_{max} and K_m:

$$v = (V_{max}[S])/(K_m + [S]) \quad (1)$$

V_{max} was converted to k_{cat} using

$$k_{cat} = V_{max}/[E] \quad (2)$$

The assays were repeated in the presence of 5 μM 14-3-3ζ to determine the kinetic parameters of the AANAT−14-3-3ζ complex.

Binding of Semisynthetic AANATs to 14-3-3ζ. Two anisotropy-based binding assays were developed to characterize the interaction of AANAT with the adaptor protein 14-3-3ζ. The first assay was a competitive binding assay (*18*) in which AANAT displaced a fluorescently labeled AANAT-derived phosphopeptide ligand (fluorescein-HN-GIPGSPGRQRRH**pT**LPANEFR-COOH) from 14-3-3ζ. These 150 μL assays contained 100 nM fluorescent peptide and were conducted in 50 mM HEPES (pH 7.5), 50 mM NaCl, 1 mM EDTA, 5 mM DTT, and 5% glycerol. To determine the K_D of the fluorescent peptide for 14-3-3ζ, the concentration of 14-3-3ζ was varied from 0.5 to 25 μM. The protein and peptide were allowed to equilibrate for 30 min at room temperature before the anisotropy was recorded on a SPEX Fluoromax-2 spectrofluorometer (Instruments SA, Edison, NJ). The excitation wavelength was 492 nm (2 nm slit width), the emission wavelength 520 nm (4 nm slit width), and the integration time 0.5 s. Points represent an average of five measurements. The data were corrected by subtracting the anisotropy value of the free fluorescent peptide and normalized to an A_{max} of 1. The data were fit to the following equation to yield K_D and A_{max}:

$$A = (A_{max}[L])/(K_D + [L]) \quad (3)$$

In the displacement assays, the concentrations of fluorescent peptide and 14-3-3ζ were held constant at 100 nM and 5 μM, respectively (K_d = 3.2 ± 0.3 μM), and AANAT concentrations were varied. The proteins and fluorescent peptide were allowed to equilibrate for 30 min at room temperature before the anisotropy was recorded as described above.

We developed a more sensitive anisotropy-based binding assay utilizing fluorescently labeled semisynthetic 14-3-3ζ (ss-14-3-3ζ-Rh). This permitted the direct assessment of

formation of the AANAT−14-3-3ζ complex by monitoring increases in anisotropy. These 150 μL assays contained 10 nM ss-14-3-3ζ-Rh and were conducted in 50 mM HEPES (pH 7.5), 50 mM NaCl, 1 mM EDTA, 5 mM DTT, and 5% glycerol. The AANAT concentration was varied from 0.05 to 10 μM. The proteins were mixed and allowed to equilibrate for 30 min at room temperature before the anisotropy was recorded on the SPEX Fluoromax-2 spectrofluorometer. The excitation wavelength was 550 nm (5 nm slit width), the emission wavelength 580 nm (5 nm slit width), and the integration time 1 s. Points represent an average of five measurements. The data were corrected by subtracting the anisotropy value of free ss-14-3-3ζ-Rh and fit to eq 3 to yield K_D and A_{max}.

In Vitro Characterization of FRET-Labeled AANAT (Fl-AANAT-Rh). Purified Fl-AANAT-Rh was subjected to absorbance spectroscopy to determine the stoichiometric incorporation of each fluorophore. The stock protein was diluted 1:10 in storage buffer, and the absorbance spectrum was recorded from 300 to 700 nm versus a buffer blank. The molar concentration of each fluorophore was estimated from its respective extinction coefficient (rhodamine $\varepsilon_{558} = 60000\ M^{-1}\ cm^{-1}$, and fluorescein $\varepsilon_{501} = 68000\ M^{-1}\ cm^{-1}$).

To determine the intramolecular FRET efficiency, Fl-AANAT-Rh was subjected to thrombin proteolysis followed by fluorescence spectroscopy to determine the donor (fluorescein) to acceptor (rhodamine) fluorescence ratio over varying degrees of AANAT digestion. AANAT contains a single major thrombin cleavage site (*3*), making this a desirable protease for the analysis. These reactions (20 μL) were carried out in storage buffer and contained 4 μg of Fl-AANAT-Rh and 0.1−10 units of thrombin (GE Healthcare). The digestions were run in duplicate and were allowed to proceed at room temperature overnight. For each thrombin concentration, one reaction was quenched with 5 μL of 5× SDS−PAGE loading buffer and used to determine the extent of digestion via SDS−PAGE. The duplicate sample was diluted 7-fold with storage buffer and used for fluorescence spectroscopy on a SPEX Fluoromax-2 spectrofluorometer to determine the FRET ratio. Emission spectra were recorded from 500 to 700 nm with an excitation wavelength of 495 nm. The slit width was 1 nm for incident light and 1 nm for emission light.

Microinjection Studies. CHO-K1 cells (ATCC) were cultured in ATCC F-12K medium supplemented with 10% (v/v) fetal bovine serum and 100 units each of penicillin and streptomycin and incubated at 37 °C in the presence of 5% CO_2. Cells were seeded onto glass-bottom culture dishes (MatTek Corp.) and used for microinjection within 24 h (60−70% confluence). Cells were washed twice with Hank's balanced salt solution buffer and treated with 50 μM Forskolin (Calbiochem) or 1 μM MG132 (Sigma) as indicated prior to microinjection.

For microinjection and imaging, the culture dish was warmed at 37 °C. The sample (0.35 mg/mL Fl-AANAT-Rh and 1.4 mg/mL 14-3-3ζ) was loaded into Femtotip II capillaries (Eppendorf) and injected into the cells using Eppendorf Micromanipulator 5171 and Eppendorf Transjector 5246 instruments. A minimum of eight cells were treated and imaged for each dish, and at least three dishes were imaged for each of the three conditions (untreated, Forskolin-treated, and MG132-treated).

Cells were imaged on a Zeiss Axiovert 200M microscope with a 40×/1.3NA oil-immersion objective lens and cooled charge-coupled device camera (MicroMax BFT512, Roper Scientific) controlled by Metafluor version 6.2 (Molecular Devices). Dual emission ratio imaging used a 480 DF30 excitation filter, a 505 DRLP dichroic mirror, and two emission filters (535 DF45 for fluorescein and 653 DF95 for rhodamine) alternated by a Lamda 10-2 filter changer (Sutter Instruments). The exposure time was 200 ms, and images were taken every 60 s. Fluorescent images were background-corrected by subtracting fluorescence intensities of noninjected cells or background with no cells from the emission intensities of fluorescent cells microinjected with sample. The ratios of rhodamine to fluorescein emissions were then calculated at different time points and normalized by dividing all ratios by the emission ratio at the start of the imaging experiment.

FRET efficiency was determined by acceptor photobleaching. Rhodamine was photobleached at the end of the experiment by intense illumination with a 568/55 filter for 20 min. Fluorescein fluorescence intensities before (F_{da}) and after (F_d) rhodamine photobleaching and eq 4 were used to calculate FRET efficiency:

$$E = 1 - F_{da}/F_d \quad (4)$$

RESULTS

Preparation of Semisynthetic Proteins. There are two general strategies for protein semisynthesis employed here (Scheme 1). For C-terminal ligations (also known as expressed protein ligation), an intein is used to install a C-terminal thioester in the recombinant protein piece for ligation to a synthetic peptide containing an N-teminal Cys (*14*). For N-terminal ligations, the requisite N-terminal Cys is generated in the recombinant protein piece by protease cleavage (Factor Xa or Sumo), and this is ligated to a synthetic peptide containing a C-terminal thioester (*13*). The synthetic peptide thioesters were formed using a postassembly strategy as reported previously (*13*). In prior studies (*13, 14*), the N- and C-termini were truncated for synthetic ease, but in this investigation, full-length AANAT proteins were prepared to attempt to better recapitulate the physiologically relevant forms. In the previous work (*13, 14*), it was shown that site-specific incorporation of phosphono-Ala (nonhydrolyzable pSer/pThr mimic) could be achieved by ligation of synthetic peptide thioester amino acids 1−33 to recombinant protein fragment amino acids 34−199 or recombinant protein thioester fragment 34−199 to synthetic peptide 200−207. Building on this initial research, we have carried out successive ligations as displayed in Scheme 1 to generate singly and doubly phosphorylated semisynthetic proteins [ss-pT31 and ss-pT31-p205 (Figure 1)]. In this procedure, AANAT 34−199 is subcloned into an intein vector which also contains an N-terminal Factor Xa cleavage site. Ligation to the protein thioester is performed prior to liberation of the N-Cys at position 34 by site-specific proteolysis. As described previously (*13*), the N-terminal ligation necessitated the insertion of two amino acid residues, Gly-Cys, to allow for both Factor Xa cleavage and efficient chemical ligation, presumably because of the need for flexibility in this region. Since it is possible that this Gly-Cys insertion (between amino acids 33 and 34) and/or

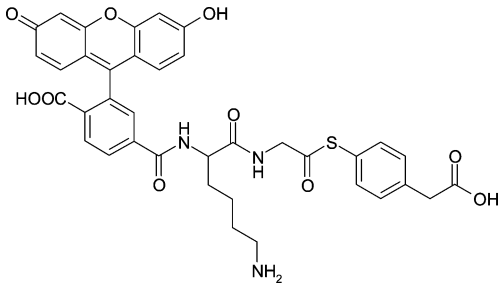

FIGURE 3: Fluorescein thioester reagent used to FRET label AANAT.

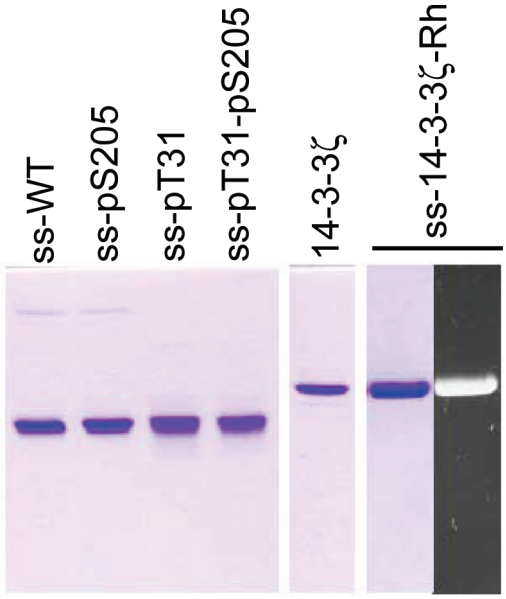

FIGURE 4: SDS−PAGE analysis of proteins used in this study. Proteins (2.5−5 μg) were denatured in SDS−PAGE loading buffer and separated on 12% gels. Proteins were visualized with Coomassie blue staining and where applicable by UV transillumination.

N-terminal ligation could generate aberrantly behaving AANAT displaying subtly altered interactions with 14-3-3ζ, we also prepared semisynthetic AANATs lacking this insertion (ss-WT and ss-pS205) as well as recombinantly GC-inserted AANAT [ss-GC-insert (Figure 1)]. These were then phosphorylated using classical protein kinase A treatment (Figure 2), as described previously (*3, 6*). The full range of specific semisynthetic proteins prepared and analyzed here is displayed in Figures 1 and 2. Each exhibited high purity (>90%) as determined by SDS−PAGE (representative examples shown in Figure 4) and mass spectrometric analysis.

In addition to generating semisynthetic phosphorylated AANATs, we also used a three-piece ligation approach (*19*) to fluorescently label AANAT on both its N- and C-termini [Fl-AANAT-Rh (Scheme 2)] with fluorescein and rhodamine, respectively (Figure 1). This dual fluorescently labeled protein Fl-AANAT-Rh was designed to examine the potential for intramolecular FRET within AANAT for stability studies. Generation of Fl-AANAT-Rh required employing a previously prepared Cys-rhodamine dipeptide for C-terminal labeling and a novel thioester fluorescein compound (Figure 3) for N-terminal labeling. We also employed the Cys-rhodamine dipeptide reagent to prepare fluorescently labeled 14-3-3ζ by expressed protein ligation (Figures 1 and 4) for use in fluorescence anisotropy binding studies.

AANAT−14-3-3ζ Interaction. While prior efforts to assess the affinity of recombinant phosphorylated AANATs with recombinant 14-3-3ζ have been reported (*3*−*6*), these measurements have involved the use of immobilized proteins which have the potential to introduce surface effects that can alter interactions (*20*). We thus investigated the potential of fluorescence binding assays to make these measurements. Our initial effort involved the application of a fluorescent phosphorylated synthetic peptide derived from AANAT, fluorescein-HN-GIPGSPGRQRRH**pT**LPANEFR-COOH, which we applied in anisotropy binding studies using a competition assay. In this approach, it was found that the fluorescent phosphopeptide exhibited an apparent K_D with 14-3-3ζ of 3.2 μM (Figure 5A). We tested several of the semisynthetic phospho-AANATs as competitors of this phosphopeptide (Figure 5B), and these studies revealed that AANAT phosphorylated at Thr31 (ss-pT31 and ss-pT31-pS205) competed efficiently in the low micromolar range whereas AANAT phosphorylated at 205 (ss-pS205) exhibited reduced affinity. However, these studies were complicated by the observation of an unexpected increase in anisotropy at lower concentrations of three of the semsiynthetic AANATs (Figure 5B). While the origin of this increase is uncertain, it is possible that a population of the AANATs could be binding to the phosphopeptide−14-3-3ζ complex in a noncompetitive fashion, increasing the apparent anisotropy. Interestingly, even the unmodified AANAT (ss-WT) protein exhibited a modest ability to enhance the anisotropy of the fluorescent peptide, supporting the idea that nonclassical 14-3-3ζ or peptide interaction is involved. In any case, this complication as well as the lack of sensitivity (below the low micromolar range) stimulated us to consider another approach.

In an effort to develop a more direct binding assay, we tested ss-14-3-3ζ-Rh as an interactor for the fluorescent assay. Interestingly, addition of phosphorylated semisynthetic AANATs to a solution of ss-14-3-3ζ-Rh exhibited a concentration-dependent change in anisotropy (Figure 6), fitting well to classical ligand−receptor interaction, which allowed for measurement of K_D values. As shown in Table 1, the K_D values for ss-pT31 and ss-pT31-pS205 were 40 nM whereas the K_D for ss-p205 was 860 nM. It is noteworthy that the GC insertion was responsible for considerable affinity enhancement since ss-p205/PKA, which lacks GC insertion, exhibited a K_D of 160 nM. Consistent with this fact, the ΔC8/PKA protein displayed a K_d of 1.75 μM, 45-fold larger than that of ss-pT31 (Table 1). An important control was that ss-WT showed no evidence of anisotropy change up to 10 μM, arguing against nonspecific effects as a source of the fluorescence change. Comparing the results of ss-p205, ΔC8/PKA, and ss-p205/PKA, we find that the dual phosphorylation shows partial additivity in 14-3-3ζ binding in the non-GC-inserted context.

It is well-established that 14-3-3ζ exists as a stable homodimer (*21*). There are at least two potential models for how dual phosphorylation of AANAT could enhance affinity. In the first model, two doubly phosphorylated AANATs could bind to one ss-14-3-3ζ-Rh dimer, each AANAT binding to a separate ss-14-3-3ζ-Rh monomeric subunit. In the second model, one doubly phosphorylated AANAT could bind to a single ss-14-3-3ζ-Rh dimer, with each phosphorylated group binding to component ss-14-3-3ζ-Rh subunits. Evidence favoring the second model comes from examination

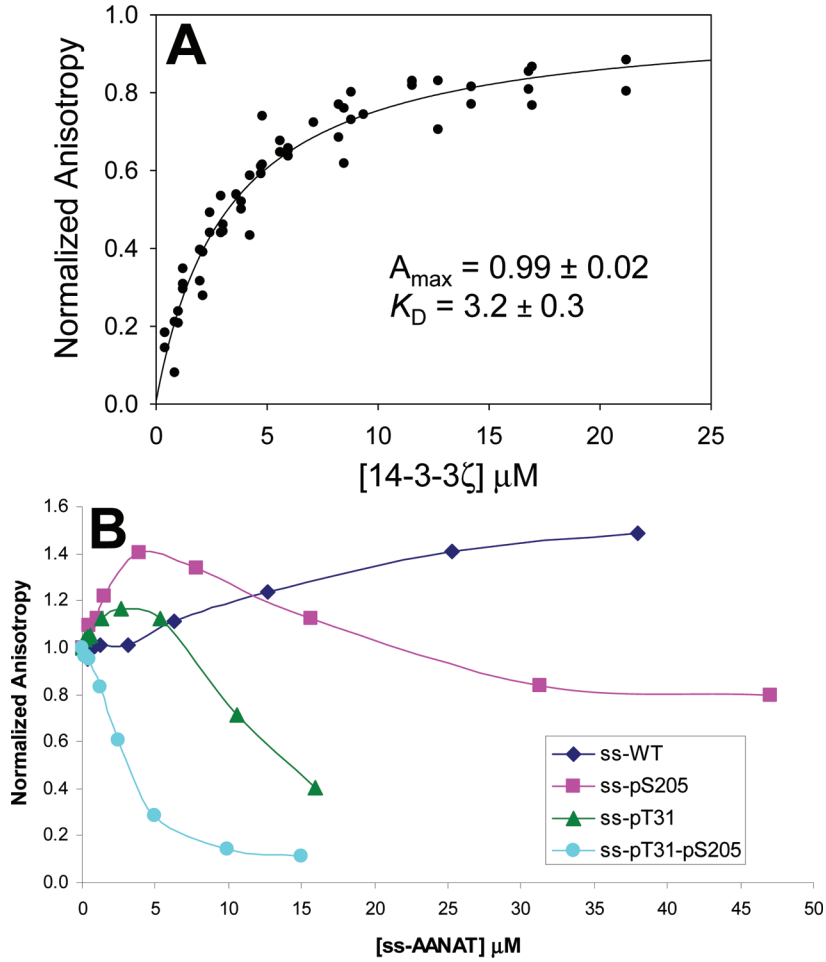

FIGURE 5: Competitive binding assay. (A) K_D determination of fluorescein-HN-GIPGSPGRQRRH**pT**LPANEFR-COOH for 14-3-3ζ. The 150 μL assays contained 100 nM fluorescent peptide, and the concentration of 14-3-3ζ was varied from 0.5 to 25 μM. Protein and peptide were incubated for 30 min at room temperature in 50 mM HEPES (pH 7.5), 50 mM NaCl, 1 mM EDTA, 5 mM DTT, and 5% glycerol before the anisotropy was recorded on a SPEX Fluoromax-2 spectrofluorometer [excitation at 492 nm (2 nm), emission at 520 nm (4 nm)]. (B) Displacement of fluorescein-HN-GIPGSPGRQRRH**pT**LPANEFR-COOH from 14-3-3ζ by semisynthetic AANATs. The 150 μL assays contained 100 nM fluorescent peptide and 5 μM 14-3-3ζ, and the concentration of semisynthetic AANAT was varied. Proteins and peptide were incubated for 30 min at room temperature in 50 mM HEPES (pH 7.5), 50 mM NaCl, 1 mM EDTA, 5 mM DTT, and 5% glycerol before the anisotropy was recorded as described for panel A.

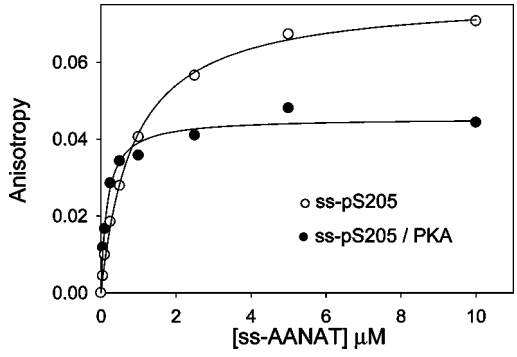

FIGURE 6: Direct binding assay. Binding of semisynthetic AANATs to 14-3-3ζ-Rh was directly monitored via anisotropy. The 150 μL assays contained 10 nM 14-3-3ζ-Rh, and the concentration of semisynthetic AANAT was varied from 0.05 to 10 μM. The proteins were incubated for 30 min at room temperature in 50 mM HEPES (pH 7.5), 50 mM NaCl, 1 mM EDTA, 5 mM DTT, and 5% glycerol before the anisotropy was recorded on a SPEX Fluoromax-2 spectrofluorometer [excitation at 550 nm (5 nm), emission at 580 nm (5 nm)]. The plot shows representative data for (○) ss-pS205 and (●) ss-pS205/PKA fit to the equation $A = (A_{max}[L])/(K_D + [L])$.

Table 1: Analysis of Binding of Semisynthetic AANATs to 14-3-3ζ-Rh

protein	K_D(14-3-3ζ) (μM)	A_{max}
ss-WT	>10.0	not available
ss-pS205	0.86 ± 0.04	0.0771 ± 0.0011
ss-pS205/PKA	0.16 ± 0.02	0.0454 ± 0.0013
ss-pT31	0.04 ± 0.01	0.0520 ± 0.0016
ss-pT31-pS205	0.04 ± 0.01	0.0519 ± 0.0011
ΔC8/PKA	1.79 ± 0.36	0.0794 ± 0.0061

of the magnitude of the anisotropy effects. Whereas the monophosphorylated AANATs exhibited a maximal anisotropy change of ~0.078, diphosphorylated ss-p205/PKA displayed a maximal change of 0.045 (Figure 6 and Table 1). In general, it is assumed that a relative increase in anisotropy correlates positively with the physical size of the complexes. These results suggest that, for the monophosphorylated AANATs (lacking unnatural GC insertion), two molecules bind to one ss-14-3-3ζ-Rh dimer, resulting in a larger anisotropic perturbation, whereas only one molecule of diphosphorylated ss-p205/PKA binds to the ss-14-3-3ζ-Rh dimer, giving rise to the smaller anisotropy change.

Phospho-AANAT Acetyltransferase Activity Influence of 14-3-3ζ. Analysis of the effect of 14-3-3ζ on the acetyltransferase activity of phosphorylated AANATs was also determined. In previous studies, interaction of 14-3-3ζ with

Table 2: Kinetic Analysis of Semisynthetic AANATs

protein	k_{cat} (s^{-1})	K_m(tryptamine) (μM)	k_{cat}/K_m (μM^{-1} s^{-1})
ss-WT	17.3 ± 1.2	60.1 ± 13.5	0.29
ss-WT and 14-3-3ζ	20.3 ± 0.8	95.7 ± 13.3	0.21
ss-WT/PKA	25.9 ± 0.6	105.8 ± 7.9	0.24
ss-WT/PKA and 14-3-3ζ	8.8 ± 0.5	16.3 ± 4.8	0.54
ss-pS205	19.6 ± 0.7	73.5 ± 8.8	0.27
ss-pS205 and 14-3-3ζ	22.9 ± 1.5	87.8 ± 19.2	0.26
ss-pS205/PKA	18.9 ± 0.3	87.7 ± 5.2	0.22
ss-pS205/PKA and 14-3-3ζ	6.3 ± 1.2	16.0 ± 12.0	0.39
ss-pT31	17.8 ± 0.4	72.5 ± 5.4	0.25
ss-pT31 and 14-3-3ζ	19.8 ± 1.3	85.6 ± 19.0	0.23
ss-pT31-pS205	16.5 ± 0.7	65.4 ± 10.7	0.25
ss-pT31-pS205 and 14-3-3ζ	17.3 ± 0.4	51.7 ± 4.7	0.33
ss-pT31-pS205/PKA	18.2 ± 1.1	115.8 ± 18.7	0.16
ss-pT31-pS205/PKA and 14-3-3ζ	18.1 ± 1.4	79.8 ± 17.9	0.23
ΔC8/PKA	18.2 ± 0.7	252.9 ± 30.7	0.07
ΔC8/PKA and 14-3-3ζ	28.0 ± 2.4	54.8 ± 21.2	0.51
ss-GC-Insert/PKA	16.2 ± 0.5	80.7 ± 7.4	0.20
ss-GC-Insert/PKA and 14-3-3ζ	15.6 ± 0.5	46.9 ± 5.0	0.33

pThr31-modified AANAT was suggested to have a stimulatory effect on catalysis (primarily lowering of K_m for tryptamine), whereas 14-3-3ζ binding to pS205-modified AANAT showed modest inhibition (*3*−*6*). Recapitulating the pThr31 data, we found 14-3-3ζ addition led to 5-fold reduction in the tryptamine K_m and a 7-fold enhanced catalytic efficiency (k_{cat}/K_m) for ΔC8/PKA (Table 2). Interestingly, the effect of 14-3-3ζ on ss-pS205 was negligible for either K_m or k_{cat}/K_m [<20% change (Table 2)], in contrast to prior studies (*6*). However, experiments with doubly phosphorylated AANAT, pS205/PKA, showed that 14-3-3ζ induced a 5-fold tryptamine K_m reduction that was largely offset by a k_{cat} decrease such that the catalytic efficiency (k_{cat}/K_m) exhibited a <2-fold effect (Table 2).

In contrast, studies with semisynthetic AANATs ss-pT31 or ss-pT31-pS205 revealed surprisingly small effects [≤30% (Table 2)] of 14-3-3ζ on tryptamine K_m or k_{cat}/K_m. This unexpected contrast with the ΔC8 and pS205/PKA results suggests that either the N-terminal ligation production method or the fact of GC insertion itself affects the interaction of the phosphorylated AANAT with 14-3-3ζ. To distinguish between these possibilities, we tested the impact

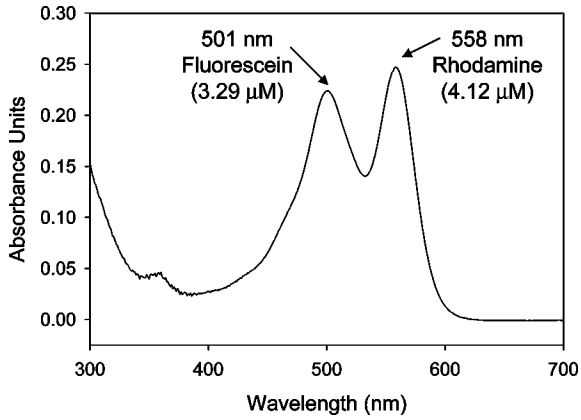

FIGURE 7: Spectral analysis of Fl-AANAT-Rh. A stock Fl-AANAT-Rh solution was diluted 1:10 in 50 mM HEPES (pH 7.5), 150 mM NaCl, 1 mM EDTA, 10% glycerol, and 10 mM DTT, and the absorbance spectrum was recorded from 300 to 700 nm vs a buffer blank. The molar concentration of each fluorophore was calculated from its respective extinction coefficient (rhodamine $\varepsilon_{558} = 60000$ M^{-1} cm^{-1}, and fluorescein $\varepsilon_{501} = 68000$ M^{-1} cm^{-1}).

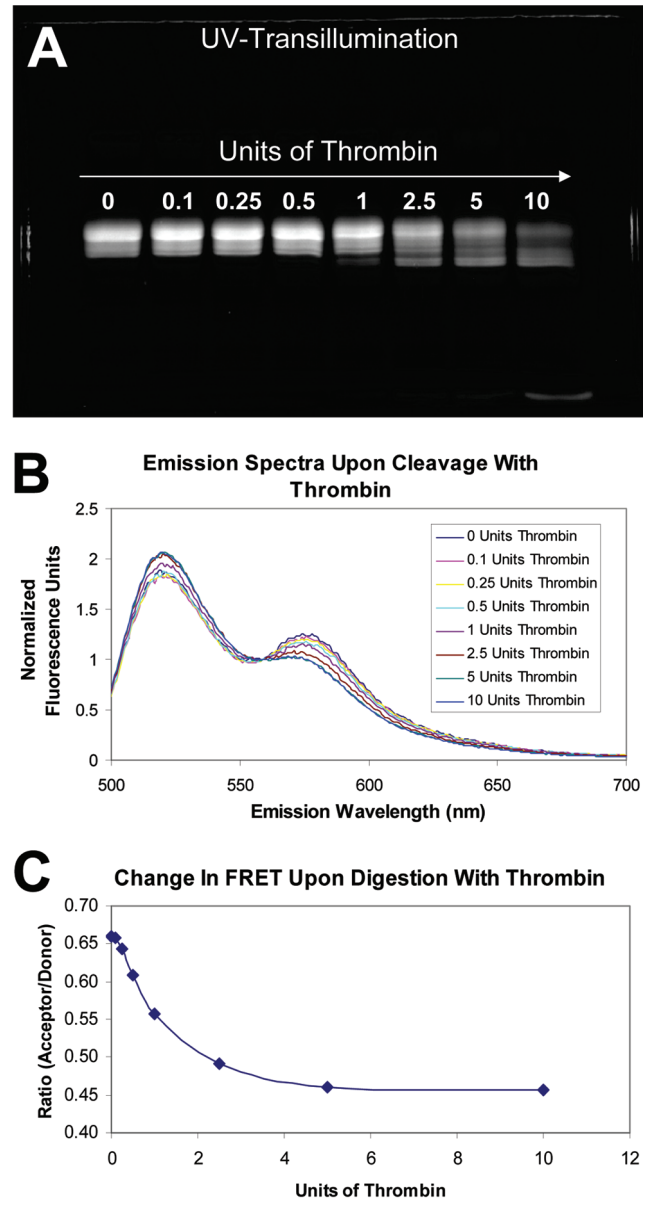

FIGURE 8: Thrombin digestion of Fl-AANAT-Rh. Fl-AANAT-Rh (4 μg) was treated with 0.1−10 units of thrombin overnight at room temperature. The reactions (20 μL) were carried out in 50 mM HEPES (pH 7.5), 150 mM NaCl, 1 mM EDTA, 10% glycerol, and 10 mM DTT. (A) Samples were denatured in SDS−PAGE loading buffer, separated on a 12% gel, and visualized via UV transillumination. (B and C) Duplicate samples were diluted 7-fold with 50 mM HEPES (pH 7.5), 150 mM NaCl, 1 mM EDTA, 10% glycerol, and 10 mM DTT and used for fluorescence spectroscopy on a SPEX Fluoromax-2 spectrofluorometer to determine the FRET ratio. Emission spectra were recorded from 500 to 700 nm with an excitation wavelength of 495 nm. The slit width was 1 nm for incident light and 1 nm for emission light. Spectra in panel B were adjusted such that the relative fluorescence was normalized to that observed at 559 nm. Panel C shows the replot of the units of thrombin vs the FRET ratio (fluorescein/donor emission to rhodamine/acceptor emission).

of 14-3-3ζ on the acetyltransferase activity of ss-GC-Insert/PKA, which was not subject to chemical manipulation of its N-terminus. The behavior of ss-GC-Insert/PKA acetyltransferase activity was nearly identical to that of ss-pT31-pS205 (Table 2), implying that the GC insert, rather than being an artifact of the ligation procedure, is the basis for the loss of a 14-3-3ζ effect.

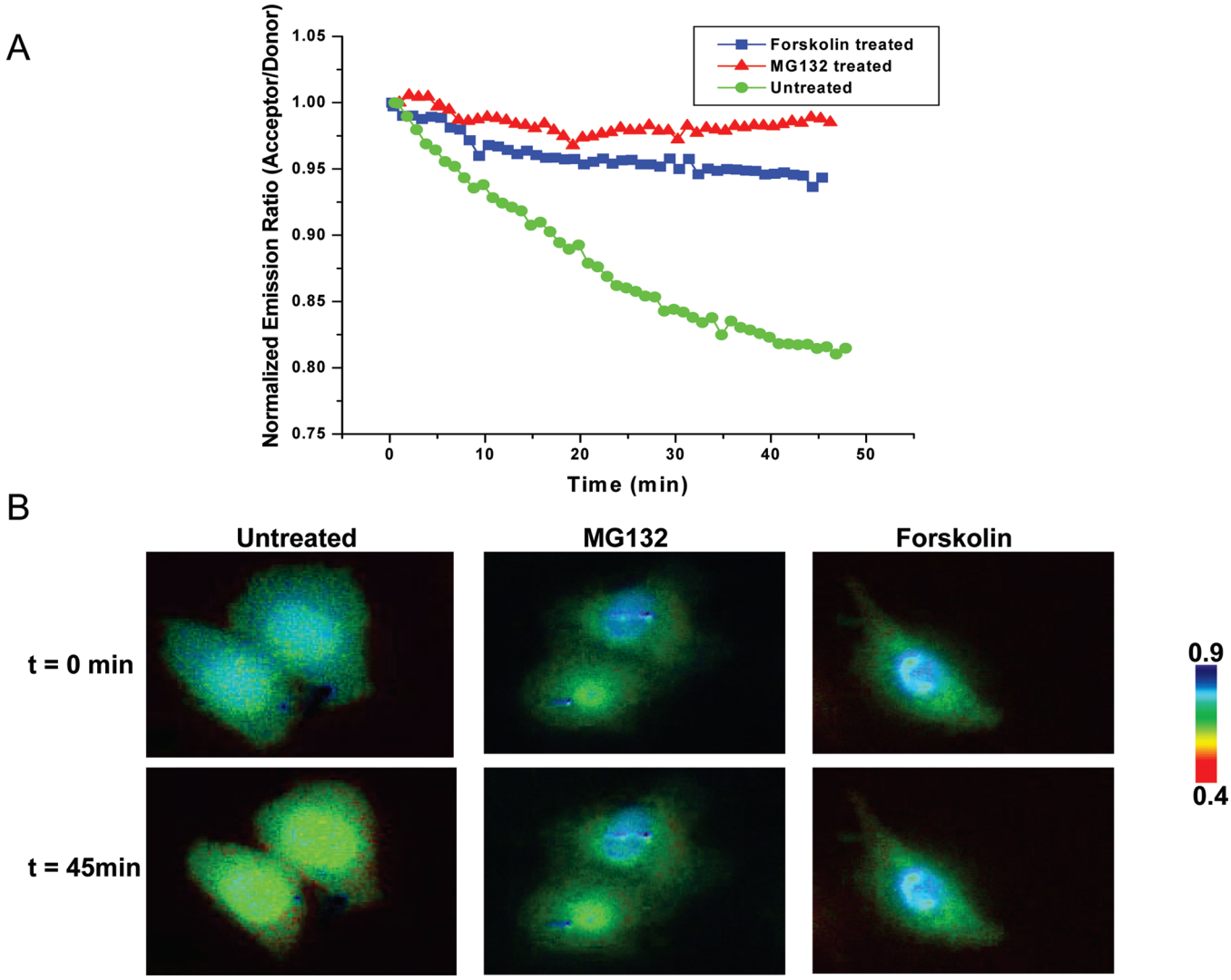

FIGURE 9: Cell microinjection experiments. (A) Time course of emission ratios after microinjection of Fl-AANAT-Rh and 14-3-3ζ under different conditions (indicated) based on an average of at least eight cells. (B) Pseudocolor images of emission ratios (acceptor:donor) for representative cells visualized by fluoroscence microscopy immediately after injection and 45 min later. Cells were treated as indicated prior to injection.

FRET Analysis of AANAT Labeled with Fluorescein and Rhodamine (Fl-AANAT-Rh). The dual fluorescently labeled AANAT, Fl-AANAT-Rh (Figure 7), was excited in its fluorescein absorbance range and showed evidence of fluorescence energy transfer (FRET) from its N-terminal fluorescein donor to its C-terminal rhodamine acceptor. While this apparent FRET activity was not affected by substrate binding (data not shown), it was clearly reduced after protease treatment with either thrombin (Figure 8) or trypsin (data not shown). In this way, the degree of thrombin proteolysis correlated nicely with the fluorescence change as shown in Figure 8. An increasing level of thrombin, known to cleave AANAT near its N-terminus (*3*), from 0.1 to 10 units induced elevated fluorescence emission of fluorescein, as expected for a loss of FRET (Figure 8). This FRET effect was confirmed by plotting the thrombin level versus the rhodamine acceptor to fluorescein donor fluorescence ratio as shown in Figure 8.

We next undertook microinjection studies to examine the potential to visualize the kinetics of AANAT degradation in live cells. In these experiments, Fl-AANAT-Rh was injected along with excess recombinant 14-3-3ζ into CHO cells, and the fluorescence acceptor:donor ratio in individual cells was monitored over time using fluorescence microscopy (Figure 9). This observed acceptor:donor ratio was interpreted as degradation of AANAT due to proteolysis, previously observed to occur on this time scale. The initial cellular FRET efficiency of Fl-ANAAT-Rh was measured by acceptor photobleaching as 60 ± 6% ($n = 5$) (*22, 23*).

To further investigate this change, we pretreated the CHO cells with the adenylyl cyclase activating compound forskolin prior to microinjection, which is predicted to stimulate phosphorylation of AANAT by protein kinase A (*24*). Forskolin pretreatment significantly attenuated the FRET change in CHO cells, consistent with the predicted stabilization of AANAT upon phosphorylation and complexation with 14-3-3ζ (Figure 9). We also tested the effects of the proteasome inhibitor MG132 (*25*) on AANAT FRET. Prior studies had suggested that proteasomal action plays a role in AANAT breakdown when it is unphosphorylated (*7*). Indeed, MG132 also blocked loss of FRET in microinjected CHO cells (Figure 9), consistent with a role for proteasome-mediated degradation in the regulation of AANAT stability in a live cell assay.

DISCUSSION

While prior studies had demonstrated the potential for 14-3-3ζ-mediated catalytic activation of phosphorylated AANAT by engagement (*3*−*6*), the studies here provide new insights into the scope and mechanism of this activation. It was confirmed that a single phosphorylation at Thr31, but not Ser205, can activate AANAT through 14-3-3ζ interaction by lowering the K_m of tryptamine. However, double phosphorylation largely abolishes this activation in that the k_{cat} decrease offsets the K_m change. On the basis of the fluorescence anisotropy studies, a potential mechanistic basis for this change involves dual engagement of the doubly phosphorylated AANAT into each subunit of one 14-3-3ζ dimer. We have also discovered that the Thr31 phosphorylation effects on the interaction of AANAT with 14-3-3ζ and catalysis are very sensitive to N-terminal Gly-Cys insertion, performed to aid in semisynthesis. Although this N-terminal region of AANAT has been assumed to be quite flexible (*3*−*6*), it is clear that functional perturbation by residue insertion can be transmitted to active site interactions. These findings indicate the precise requirements of the native N-terminal AANAT conformation for phosphorylation-induced protein−protein interaction to allosterically regulate acetyltransferase activity.

A new approach was developed which allows for solution phase affinity of 14-3-3ζ binding to phosphorylated AANAT to be determined. This assay should be adaptable to other protein systems. We were surprised by the finding that Ser205 phosphorylation of AANAT results in a tighter interaction with 14-3-3ζ (0.86 μM) than does pThr31-AANAT (1.75 μM), despite the fact that the pThr31 modification occurs in a canonical 14-3-3ζ binding sequence whereas Ser205 does not. These results underscore the importance of the protein context in interpreting peptide consensus binding information. On the basis of the AANAT Gly-Cys insertion binding and catalysis data, the comparatively weak interaction involving pThr31-AANAT can perhaps be due to the competitive influence of the native residues C-terminal to Thr31 which presumably interact internally with the AANAT structure in a manner that modulates catalytic activity. The partial additivity of effects of pThr31 and pSer205 in AANAT binding to 14-3-3ζ results in a 5-fold enhanced affinity of the doubly modified AANAT over the pSer205-AANAT protein. This is far less than the maximal, theoretical additive value of dual engagement which might be expected to cause a 10^6-fold effect if each phosphorylation site achieved optimal engagement in 14-3-3ζ dimer subunits (*27*). These findings suggest that energetic strain is introduced in the dual engagement model which prevents realization of the full energetic potential.

Sequential native chemical ligation was used to generate a protein labeled with a FRET pair at its N- and C-termini, the second time (*19*) this has been performed on a protein to the best of our knowledge. In the prior study, Cotton and Muir generated semisynthetic CrkII protein containing a fluorescein and rhodamine at either terminus, and a small (3%) FRET change was observed upon tyrosine phosphorylation in vitro, indicative of a conformational change (*19*). Here we have used FRET analysis of the semisynthetic AANAT protein to assess proteolytic stability in vitro and in cell culture. The fluorescence analysis of small molecule FRET pairs is a well-established application for protease assays on short synthetic peptides (*28*), but in this study, we have extended the approach to larger proteins. The robust FRET change has allowed us to confirm in live cells the rather rapid kinetics of AANAT degradation in the absence of kinase activation by forskolin or proteasome inhibition by MG132. The possibility that loss of the FRET signal is due to protein unfolding exists; however, prior results obtained via immunocytochemistry with fixed cells showed loss of epitope, which correlates with the findings described here (*13, 14*). Furthermore, unfolded proteins tend to be rapidly degraded in the cell. The advantage of showing this prior to cellular fixation rules out that such a perturbation was influencing protein behavior. Another advantage of our approach as opposed to the more typical CFP−YFP fusion method (*29*) (which would triple the size of AANAT) is the small size of the synthetic fluorophore attachments which might be expected to be less perturbing with respect to cellular interactions. In future experiments, we hope to explore this FRET AANAT technique using a wider range of pharmacologic conditions to discover new substances which influence melatonin regulation.

ACKNOWLEDGMENT

We are very grateful to J. Culhane, D. Klein, J. Liu, and S. Ganguly for sharing ideas and helpful discussions.

REFERENCES

1. Klein, D. C., Coon, S. L., Roseboom, P. H., Weller, J. L., Bernard, M., Gastel, J. A., Zatz, M., Iuvone, P. M., Rodriquez, I. R., Begay, V., Falcon, J., Cahill, G. M., Cassone, V. M., and Baler, R. (1997) The Melatonin Rhythm-generating enzyme: Molecular regulation of serotonin N-acetyltransferase in the pineal gland. *Recent Prog. Horm. Res. 52*, 307–357.
2. Klein, D. C. (2007) Arylalkylamine N-acetyltransferase: "The timezyme". *J. Biol. Chem. 282*, 4233–4237.
3. Ganguly, S., Gastel, J. A., Weller, J. L., Schwartz, C., Jaffe, H., Namboodiri, M. A., Coon, S. L., Hickman, A. B., Rollag, M., Obsil, T., Beauverger, P., Ferry, G., Boutin, J. A., and Klein, D. C. (2001) Role of a pineal cAMP-operated arylalkylamine N-acetyltransferase/14-3-3-binding switch in melatonin synthesis. *Proc. Natl. Acad. Sci. U.S.A. 98*, 8083–8088.
4. Obsil, T., Ghirlando, R., Klein, D. C., Ganguly, S., and Dyda, F. (2001) Crystal structure of the 14-3-3ζ:serotonin N-acetyltransferase complex. A role for scaffolding in enzyme regulation. *Cell 105*, 257–267.
5. Klein, D. C., Ganguly, S., Coon, S. L., Shi, Q., Gaildrat, P., Morin, F., Weller, J. L., Obsil, T., Hickman, A., and Dyda, F. (2003) 14-3-3 proteins in pineal photoneuroendocrine transduction: How many roles? *J. Neuroendocrinol. 15*, 370–377.
6. Ganguly, S., Weller, J. L., Ho, A., Chemineau, P., Malpaux, B., and Klein, D. C. (2005) Melatonin synthesis: 14-3-3-dependent activation and inhibition of arylalkylamine N-acetyltransferase mediated by phosphoserine-205. *Proc. Natl. Acad. Sci. U.S.A. 102*, 1222–1227.
7. Gastel, J. A., Roseboom, P. H., Rinaldi, P. A., Weller, J. L., and Klein, D. C. (1998) Melatonin production: Proteasomal proteolysis in serotonin N-acetyltransferase regulation. *Science 279*, 1358–1360.
8. Ferry, G., Mozo, J., Ubeaud, C., Berger, S., Bertrand, M., Try, A., Beauverger, P., Mesangeau, C., Delagrange, P., and Boutin, J. A. (2002) Characterization and regulation of a CHO cell line stably expressing human serotonin N-acetyltransferase (EC 2.3.1.87). *Cell. Mol. Life Sci. 59*, 1395–1405.
9. Dawson, P. E., and Kent, S. B. (2000) Synthesis of native proteins by chemical ligation. *Annu. Rev. Biochem. 69*, 923–960.
10. Erlanson, D. A., Chytil, M., and Verdine, G. L. (1996) The leucine zipper domain controls the orientation of AP-1 in the NFAT.AP-1.DNA complex. *Chem. Biol. 3*, 981–991.

11. Muir, T. W., Sondhi, D., and Cole, P. A. (1998) Expressed protein ligation: A general method for protein engineering. *Proc. Natl. Acad. Sci. U.S.A. 95*, 6705–6710.
12. Evans, T. C., Jr., Benner, J., and Xu, M. Q. (1998) Semisynthesis of cytotoxic proteins using a modified protein splicing element. *Protein Sci. 7*, 2256–2264.
13. Zheng, W., Zhang, Z., Ganguly, S., Weller, J. L., Klein, D., and Cole, P. A. (2003) Cellular stabilization of the melatonin rhythm enzyme induced by non-hydrolyzable phosphonate incorporation. *Nat. Struct. Biol. 10*, 1054–1057.
14. Zheng, W., Schwarzer, D., LeBeau, A., Weller, J. L., Klein, D. C., and Cole, P. A. (2005) Cellular stability of serotonin N-acetyltransferase conferred by phosphono-difluoromethylene alanine (Pfa) substitution for Ser205. *J. Biol. Chem. 280*, 10462–10467.
15. Scheibner, K. A., Zhang, Z., and Cole, P. A. (2003) Merging FRET and expressed protein ligation to analyze protein-protein interactions. *Anal. Biochem. 317*, 226–232.
16. Backes, B. J., and Ellman, J. A. (1999) An Alkanesulfonamide "Safey-Catch" Linker for Solid-Phase Synthesis. *J. Org. Chem. 64*, 2322–2330.
17. DeAngelis, J., Gastel, J., Klein, D. C., and Cole, P. A. (1998) Kinetic analysis of the catalytic mechanism of serotonin *N*-acetyltransferase. *J. Biol. Chem. 273*, 3045–3050.
18. Wu, M., Coblitz, B., Shikano, S., Long, S., Cockrell, L. M., Fu, H., and Li, M. (2006) SWTY: A general peptide probe for homogeneous solution binding assay of 14-3-3 proteins. *Anal. Biochem. 349*, 186–196.
19. Cotton, G. J., and Muir, T. W. (2000) Generation of a dual-labeled fluorescence biosensor for Crk-II phosphorylation using expressed protein ligation. *Chem. Biol. 7*, 253–261.
20. Ladbury, J. E., Lemmon, M. A., Zhou, M., Green, J., Botfield, M. C., and Schlessinger, J. (1995) Measurement of the binding of tyrosyl phosphopeptides to SH2 domains: A reappraisal. *Proc. Natl. Acad. Sci. U.S.A. 92*, 3199–3203.
21. Fu, H., Subramanian, R. R., and Masters, S. C. (2000) 14-3-3 Proteins: Structure, function, and regulation. *Annu. Rev. Pharmacol. Toxicol. 41*, 523–533.
22. Miyawaki, A., and Tsien, R. Y. (2000) Monitoring protein conformations and interactions by fluoescence resonance energy transfer between mutants of green fluorescent protein. *Methods Enzymol. 327*, 472–500.
23. Zhang, J., Campbell, R. E., Ting, A. Y., and Tsien, R. Y. (2002) Creating new fluorescent probes for cell biology. *Nat. Rev. Mol. Cell Biol. 3*, 906–918.
24. Sunahara, R. K., Dessauer, C. W., and Gliman, A. G. (1996) Complexity and diversity of mammalian adenylyl cyclases. *Annu. Rev. Pharmacol. Toxicol. 36*, 461–480.
25. Lee, D. H., and Goldberg, A. L. (1998) Proteasome inhibitors: Valuable new tools for cell biologists. *Trends Cell Biol. 8*, 397–403.
26. Tzivion, G., and Avruch, J. (2002) 14-3-3 proteins: Active cofactors in cellular regulation by serine/threonine phosphorylation. *J. Biol. Chem. 277*, 3061–3064.
27. Christensen, T., Gooden, D. M., Kung, J. E., and Toone, E. J. (2003) Additivity and the physical basis of multivalency effects: A thermodynamic investigation of the calcium EDTA interaction. *J. Am. Chem. Soc. 125*, 7357–7366.
28. George, J., Teear, M. L., Norey, C. G., and Burns, D. D. (2003) Evaluation of an imaging platform during the development of a FRET protease assay. *J. Biomol. Screening 8*, 72–80.
29. Pollok, B. A., and Heim, R. (1999) Using GFP in FRET-based applications. *Trends Cell Biol. 9*, 57–60.

BI801189D